Iran J Sci Technol Trans Sci (2019) 43:1327–1336
https://doi.org/10.1007/s40995-018-0548-2

RESEARCH PAPER

# Despeckling of SAR Images by Finding the Expected Values Using the Probability Distribution of Speckle

Sarungbam Bonny[1] · Yambem Jina Chanu[2] · Khumanthem Manglem Singh[2]

Received: 17 August 2017 / Accepted: 19 March 2018 / Published online: 12 July 2018


**Abstract**
Synthetic aperture radar (SAR) images are contaminated by multiplicative speckle noise, which reduces the contrast and resolution of the images. To improve the quality and the performance of quantitative image analysis, speckle reduction is a prerequisite for SAR images. In this paper, a new method is proposed by calculating the expected value of all the pixel elements in the window with respect to the centre pixel. The weighted mean of all the expected values in the window replaces the centre pixel. The weights are calculated according to the height of the probability distribution. Thus, the expected value which has higher probability has more weightage. The proposed method is applied to the air-borne and space-borne SAR images. By comparing with some well-known filters, the obtained results demonstrate that the proposed method is able to reduce the noise effectively with accurately preserving edges and fine details of the images.

**Keywords** SAR image · Speckle noise · Speckle filter · Image filter

## 1 Introduction

Speckle is caused by random interference of the backscattered electromagnetic waves due to the roughness of the imaged surface (Goodman 1976). Synthetic aperture radar (SAR) image is degraded by the speckle due to the coherent interference of waves reflected from the imaged surface (Novak and Burl 1990; Dainty 1977). The appearance of speckle depends on the structure of the imaged surface and various imaging parameters. Speckle is generally considered to be multiplicative in nature in the sense that the appearance of speckle increases with the grey level of a local area (Argenti et al. 2013). Since speckle degrades both the spatial and the contrast resolution of the image, it is considered as noise and thus, reducing the visibility of targets. It degrades performance of SAR data analysis techniques and many processing tasks. Thus, it is necessary to reduce the speckle in the SAR images (Pang et al. 2013).

Some of the widely and commonly used filters to reduce the speckle are Lee's filter (Lee 1980, 1981), Frost's filter (Frost et al. 1981), Kuan's filter (Kuan et al. 1985; Kuan et al. 1987), median filter (Pratt 1975), diffusion filter (Perona and Malik 1990) and wavelet filter (Donoho et al. 1995; Donoho 1995; Mallat 1989). Since then, many improvements of these filters have been derived. Lee's filter forms an output by a linear combination, using local statistics, of centre pixel value in a filter window with the average pixel value of the window. The Kuan's filter has the same formation with the Lee's filter, which is based on the minimum mean square error (MMSE), but with a different weighting function. The Frost's filter is an exponential shaped filter kernel which adapts to region using local statistics. It is similar to the Lee filter, but it does more smoothing in the edge area, resulting to blur edges (Lee et al. 1994). These locally based filters achieve a balance between the averaging (in homogeneous areas) and the all pass filters (at edges and features). These weighting factors depend on the local statistics of the moving

**Electronic supplementary material** The online version of this article (https://doi.org/10.1007/s40995-018-0548-2) contains supplementary material, which is available to authorized users.

✉ Sarungbam Bonny
sarungbambonny@nitmanipur.ac.in

Yambem Jina Chanu
jina@nitmanipur.ac.in

Khumanthem Manglem Singh
manglem@nitmanipur.ac.in

[1] ECE Department, NIT Manipur, Imphal, India

[2] CSE Department, NIT Manipur, Imphal, India

window. Lee, later, developed Lee-refined filter to overcome the deficiency of Lee filter (Lee 1981). This filter uses the edge-aligned windows to reduce noise near edges. Thus, it reduces the noise near the edges with preserving edges; however, computational complexity is increased (Lee et al. 1999). Lee further developed Lee-Sigma filter (Lee 1983a, b) to do more smoothing in the heterogeneous area. In this filter, only the pixel values which lie between two-sigma ranges are averaged. Though it improves in noise reduction near edges, leaves many unfiltered black pixels. To overcome the deficiencies in Lee-Sigma filter, improved Lee-Sigma filter (Lee 2009) was designed using theoretical speckle distributions and extended improved Lee-Sigma filter (Lee et al. 2015) for very high-resolution PolSAR data. These speckle filter major limitation lies on their dependency to the shape and size of the filter window. If the window is large, it will blur the edges and a small window cannot effectively reduce the noise. In (Shitole et al. 2017), a window is divided into five equal sized overlapping sub-windows, where the centre pixel is a part of each of these sub-windows. These filters are not directional; thus, smoothing on the vicinity of an edge is excluded.

Median filter is also utilized for speckle reduction in SAR imaginary (Lee et al. 1994). It is a non-linear spatial filter. It replaces the centre pixel value in a filter window by the median value of all the pixels inside that window. A single isolated pixel in the neighbourhood will not affect median value significantly. Thus, the median filter would blur the tiny details. When the number of noised pixels is larger than the half of the filter's size, filter output remains unaltered (Michailovich and Tannenbaum 2006). Thus, median filter can be considered a failure for the fully developed speckle.

Lopes proposed Maximum A Posteriori (MAP) approach for speckle reduction using appropriate model of speckle (Lopes et al. 1990a, b, 1993). Achim performed the adaptive despeckling by deriving an MAP estimator for the Rayleigh distribution to estimate the radar cross section (Achim et al. 2009).

Non local (NL)-based algorithm is also used to reduce the speckle in SAR images (Buades et al. 2005). In NL-mean filter, the output pixel value is the weighted average of all the pixels in the image. The weight assigned to a pixel depends upon the similarity between the pixel and the pixel under consideration. In (Coupé et al. 2009), the NL mean is used by introducing the Pearson distance. Deledalle designed iteratively refined weight based on both the similarity between noisy patches and the similarity of patches extracted from the previous estimate (Deledalle et al. 2009). Gomez et al. (2013) designed an algorithm to optimize a Bayesian NL-mean filter for despeckling SAR images. Though these filters enhance edges with reducing speckle, but they have difficulties in retaining subtle features. It also leads to an over smooth effect (Yousif and Ban 2013) when many less similar pixels are used for averaging. Moreover, there may be lack of similar blocks to average in some cases. In (Leonardo et al. 2014), a combination of NL mean and a statistical test based on stochastic divergences is used to reduce speckle in PolSAR imagery. Though, the NL-mean method can effectively preserve edge details and other image details, but its computational complexity is more.

Yu and Acton designed speckle reduction anisotropic diffusion filter (SRAD) using partial differential equation (Yu and Acton 2002) which is the modification of Perona and Malik anisotropic diffusion. SRAD is a non-linear filter which is based on the iterative diffusion process. SRAD filter overcomes the drawback of the window-based approach which is sensitive to the shape and size of the filter window. Thus, this filter enhances edges by allowing diffusion in directions parallel to the edge.

Wavelet transform is also widely used in the image denoising (Mallat 1989). In Simard et al. (1998), the contribution of speckle noise in the SAR images to the wavelet decomposition is analysed. Despeckling of SAR image with Bayesian wavelet shrinkage was shown by Achim et al. (2003). Based on wavelet Bayesian denoising and Markov random field, an SAR speckle reduction algorithm was proposed (Xie et al. 2002). An NL SAR image denoising algorithm was designed based on LLMMSE wavelet shrinkage by Parrilli et al. (2012). In general, in the wavelet denoising, the wavelet coefficients below the threshold value are replaced by zero as it assumes that small coefficients are of noise and large coefficients contain signal details. Thus, the choice of threshold values is complicated as it determines the efficiency of the whole denoising systems (Donoho et al. 1995; Donoho 1995).

There are strengths and limitations of all the filters and no single filter can outperforms other in all applications (Lee et al. 1994). The choice of the filter should depend upon the application, where it is used. In some applications, it is necessary to preserve fine details like edges though they inhibit smoothing near edges while in others, to completely reduce the speckle, even though it causes problems like blurring of edges and fine details. Over the years, many speckle filters have been designed which has better performance than the widely used common adaptive filters. However, the computational complexity is increased. This added complexity is not proportional to the increase in performance. Though there is an abundance SAR speckle filters available, Boxcar or Lee filter is still employed because of its simplicity (Yamamoto et al. 2013). Adaptive filters are also employed when necessary.

In this paper, a filter is proposed based on weighted averaging the expected value of all the pixel elements in

the window. For the pixel under consideration, the possible range, where the original pixel value will lie is estimated using the noise probability distribution. The expected original value of the neighbouring noised pixel is calculated with respect to the possible range of the original centre pixel, as it assumes that the probability of similarity between the neighbouring pixels and the centre pixel is high. The motivation of this idea is that the pixel under consideration will probably have similar pixels at its neighbours. The paper is organised as follows. Section 2 presents the noise model. Section 3 illustrates the proposed filter. Experimental results and conclusion are shown in Sects. 4 and 5, respectively.

## 2 Noise Model

A priori information of the speckle in the SAR images is important in the development of the proposed filtering. SAR images are formed by capturing the return signals backscattered from a small area of the resolution cell when the radar illuminates it. Each resolution cell, where the radar illuminates it, contains several scatterers. Every scatterer contributes a backscattering wave with variational phase. As the return signals are no longer coherent in phase, the received signal is a vector sum of several backscatter waves from the scatterers (Argenti et al. 2013). These backscatter waves may sum up in a constructive or destructive way, resulting in bright and dark pixel. This pixel to pixel intensity variation in SAR images which is granular in nature is termed speckle and it is given by

$$A = \sum_i A_i e^{j\phi_i}, \tag{1}$$

where $A$ is the amplitude and $\phi$ is the phase

or

$$A = \sum_i A_i(\cos\phi_i + j\sin\phi_i) \tag{2}$$

or

$$A = x + jy. \tag{3}$$

The received signal is the coherent result of different phases between scatterers. Thus, it can be seen as the complex signal whose in phase $(A\cos\phi)$ and quadrature $(A\sin\phi)$ components of the amplitude are independent. The amplitude $|A|$ is distributed as Rayleigh pdf and it is given by

$$p_A(A) = \frac{2A}{\sigma^2} e^{-\frac{A^2}{\sigma^2}}, A \geq 0 \tag{4}$$

with the mean and variance of the amplitude $|A|$ are equal to $\sigma\frac{\sqrt{\pi}}{2}$ and $(4-\pi)\sigma^2/4$, respectively. The intensity $I = x^2 + y^2$ or $A^2$ is exponentially distributed as

$$p_I(I) = \frac{1}{\sigma^2} e^{-\frac{I}{\sigma^2}} I \geq 0 \tag{5}$$

with the mean and variance of the intensity, I, are equal to $\sigma^2$ and $\sigma^4$, respectively. The mean value, for both intensity and amplitude images, is the actual information or the actual reflectance. Thus, the SAR image can be represented as the product of the mean value and the probability distribution of the received signal with mean equal to unity. In general, SAR image is described by the mathematical model as

$$z(i,j) = u(i,j) \times v(i,j), \tag{6}$$

where $z(i,j)$ is the $(i,j)$th pixel grey level of an SAR image, $u(i,j)$ is the original pixel grey level, and $v(i,j)$ is considered as a speckle fading term with mean of unity. For simplicity, the subscripts $(i,j)$ will be omitted. Thus, Eq. 6 can be rewritten as

$$z = u \times v. \tag{7}$$

The parameter $u$ is equal to the mean value of the received signal distribution.Or

$$v = \frac{z}{u}, \tag{8}$$

where $v$ is distributed as

$$p_{\mathrm{V}}(v) = up_I(uv)(\text{intensity}) \text{ or } up_{\mathrm{A}}(uv)(\text{amplitude}) \tag{9}$$

or

$$p_{\mathrm{V}}(v) = e^{-v}(\text{for intensity}) \text{or } \frac{\pi}{2} v e^{-v^2\frac{\pi}{4}}(\text{for amplitude}). \tag{10}$$

For the multi-look processed SAR images, which are formed by averaging $N$ independent spatial observations to improve the estimation of $\sigma^2$ (i.e., to reduce the speckle), the intensity image has a Chi-square distribution, that is

$$p_I(I) = \frac{N^N}{\sigma^{2N}\Gamma(N)} I^{N-1} e^{-N\frac{I}{\sigma^2}}, \tag{11}$$

where $N$ is the number of looks and $\Gamma$ (.) denotes the Gamma function. The mean value for the $N$ looks intensity maintains to $\sigma^2$ with the variance is reduced to $\frac{\sigma^4}{N}$. For the multi-look amplitude image $A_N = \sqrt{I_N}$, the speckle has a Chi distribution, given by

$$p_A(A) = \frac{2N^N}{\sigma^{2N}\Gamma(N)} A^{2N-1} e^{-N\frac{A^2}{\sigma^2}} \tag{12}$$

with the mean and variance are given by $\frac{\Gamma(N+\frac{1}{2})}{\Gamma(N)}\sqrt{\sigma^2/N}$ and $(N - \frac{\Gamma^2(N+\frac{1}{2})}{\Gamma^2(N)})\frac{\sigma^2}{N}$, respectively. The probability distribution of $v$ (noise) for the multi-look intensity and amplitude images is

$$p_V(v) = \frac{N^N v^{N-1}}{\Gamma(N)} e^{-Nv} \tag{13}$$

and

$$p_V(v) = \frac{K^{2N} 2N^N v^{2N-1}}{\Gamma(N)} e^{-Nv^2K^2}, \tag{14}$$

where $K = \frac{\Gamma(N+\frac{1}{2})}{\Gamma(N)} \sqrt{1/N}$. The model described above is valid under the assumption that the scene under consideration is characterised by distributed scatterers. In the presence of a point target, the received signal pdf becomes a Rice distribution. In this case, the received signal power is related to the single target reflection coefficient.

## 3 Proposed Method

In general, a noise filter involves replacing the central pixel in the window by the mean value of the window. It works well in the homogeneous area, but not in the high contrast area or in the presence of edges. Since all the pixels are corrupted, it is difficult to differentiate the homogeneous area from the contrast area. The proposed method calculates the expected value of all the pixels in the window $\Omega$ with respect to centre pixel. The expected value of the neighbouring pixel is its probable original value which is similar to the original centre pixel value and it is calculated as the centre pixel will probably have similar pixels at its neighbour. The weighted sum of all the expected values replaces the centre pixel as the filtered pixel. The filter output is given as

$$\hat{u}(k,l) = \sum_{i,j \int \Omega} w(i,j)\mathrm{ex}(i,j) / \sum_{i,j \int \Omega} w(i,j), \tag{15}$$

where $k,l$ is the co-ordinate of the centre pixel in the window $\Omega$, and $i,j$ denotes the co-ordinates of the neighbouring pixels in the window $\Omega$. $w$ and ex are the weightage and the expected value, respectively.

### 3.1 Calculation of the Expected Values of the Neighbouring Pixels with Respect to Centre Pixel

In Eq. 6, the SAR image is modelled as the product of the noise-free reflectivity or original pixel ($u$) with the speckle fading term or the noise ($v$) which is independent of ($u$). Thus, the parameter ($u$) has to be produced as the filter output. From Eq. (7), $u$ can be given as

$$u = \frac{z}{v}. \tag{16}$$

Since the value of $z$ is known, the probability distribution of $u$ is calculated with respect to the probability distribution of noise ($v$). Then, the probability distribution of $u$ is given by

$$p_{U(i,j)}(u) = \begin{cases} \frac{z(i,j)}{u^2} \; p_V\left(\frac{z(i,j)}{u}\right) \\ 0 \quad \text{for} u = 0 \end{cases}. \tag{17}$$

In probability theory, the expected value of a random variable is the probability-weighted average of all possible values the random variable can take. In other words, the expected value (which is a predicted value) is calculated as the integral of all possible values each multiplied by the probability of its occurrence. Its denominator value is one since the integral over the entire probability density function is one.

In this method, the expected value of the neighbouring pixel with respect to the centre pixel is the expected value of all the values which are under both the probabilities distribution of the neighbouring pixel and the centre pixel (Fig. 1). Thus, the expected value of the neighbouring pixel is its probable original value which is similar to the original centre pixel value. The expected values of the neighbouring pixels in the window with respect to the centre pixel are calculated by

$$\mathrm{ex}(i,j) = \mathrm{Ex}(i,j)/\mathrm{nom}(i,j), \tag{18}$$

where $\mathrm{Ex}(i,j)$ is the integral of all the possible values each multiplied by both the probabilities of its occurrence in the probabilities distribution of the centre pixel and the neighbouring pixel. $\mathrm{nom}(i,j)$ is the integral of the product of the probabilities of the centre pixel and the neighbouring pixel and it is used to normalise the value. They are given as below:

$$\mathrm{Ex}(i,j) = \left[ \int_0^{u_{\mathrm{upper}}} (u \times p_{U(i,j)}(u) \times p_{U(k,l)}(u)) \mathrm{d}u \right] \tag{19}$$

$$\mathrm{nom}(i,j) = \left[ \int_0^{u_{\mathrm{upper}}} (p_{U(i,j)}(u) \times p_{U(k,l)}(u)) \mathrm{d}u \right] \tag{20}$$

and $k,l$ is the co-ordinate of the centre pixel in the window $\Omega$, $i,j$ denotes the co-ordinates of the neighbouring pixels in the window $\Omega$, and the $u_{\mathrm{upper}}$ value should be maximum value of the pixel range, i.e., 1 for double data type and 255 for uint8 data type. The expected value of the centre pixel $\mathrm{ex}(k,l)$ can be taken as $3 \times 3$ mean or $3 \times 3$ median or the centre pixel itself. The use of mean $3 \times 3$ mean or $3 \times 3$ median work well in the homogeneous, but it brings blurring to the edges. To retain the fine details, the expected value $\mathrm{ex}(k,l)$ is the MMSE in a $3 \times 3$ window. The $3 \times 3$ window is used as it gives reasonably better results than other bigger sizes. In this paper, the centre pixel is used to reduce computation.

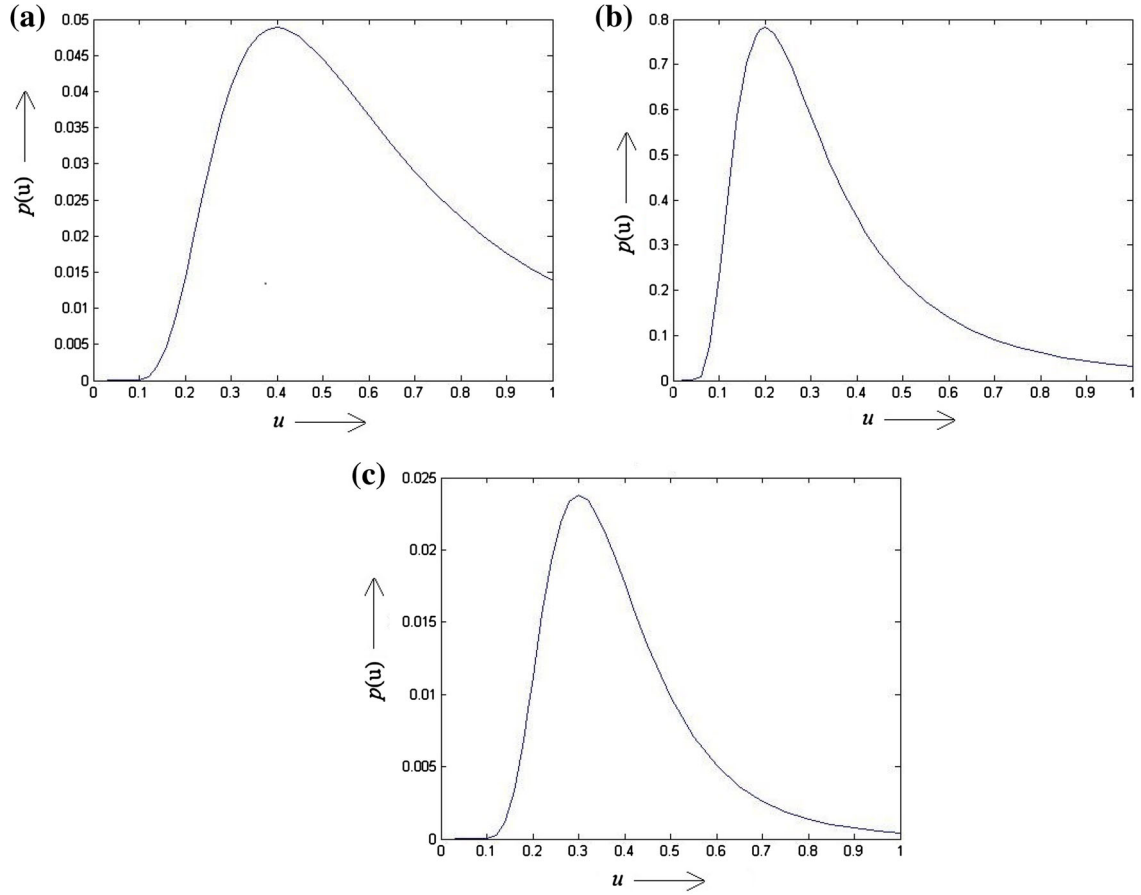


**Fig. 1** **a** Probability distribution of $u$ for the centre pixel $z(k,l)$. ($z = 0.4$). **b** Probability distribution of $u$ for the neighbouring pixel $z(i,j)$. ($z = 0.2$). **c** Product of the probability distribution of $u$ for $z = 0.4$ and $z = 0.2$. Expected value of the neighbouring pixel $z(i,j)$ $(z = 0.2)$ with respect to the centre pixel $z(k,l)$ $(z = 0.4)$ is the probability-weighted average of all possible $u$ values

The visual representation for the calculation of the expected value of the neighbouring pixel is shown in Fig. 1. Thus, the expected value of the neighbouring pixel $z(i,j)$ with respect to the centre pixel $z(k,l)$ is the expected value of the area which is under both the probability distributions of $u$ for the centre pixel $z(k,l)$ and neighbouring pixel $z(i,j)$.

Backscattering signatures of point targets follow the Rice distribution which is slightly different from that of distributed scatterers and it is observed that strong returns from point targets usually form a cluster of a large number of pixels. Thus, the pixel to be filtered in the point target would have some similar pixels in the neighbourhood and their values would be retained. The use of Rice distribution in the calculation of the expected value of the point target area would bring little difference. However, detecting the point target area in the image would add complexity. Hence, expected value in the point target area would be calculated similar to expected value in the distributed scatterers.

### 3.2 Calculation of the Weight of the Expected Values

The weight of the expected value is the probability density of the expected value in the probability distribution of the centre pixel. Thus, the weight, $w(i,j)$, is given as

$$w(i,j) = \left[ \int_{ex(i,j)-\delta}^{ex(i,j)+\delta,} p_{U(k,l)}(u)\mathrm{d}u \right], \tag{21}$$

where $\delta$ is the small value, and its value is taken 0.01 for double data type and 3 for uint8 data type. Thus, the expected value which has a higher probability of the centre will have more weightage.

## 4 Experiments and Result

Experiments are carried out on the data set acquired from both air-borne and space-borne SAR systems. The air-borne data set consists of X-band SAR image acquired over

the agricultural area, mountainous and forest area, and Ku-band SAR image acquired over the building. The space-borne data set is comprised of X-band SAR image acquired over the seaport. Thus, it consists different scattering mechanisms of the image surfaces such as specular scattering from the building block, surface scattering from the ocean areas, and volume scattering from the agricultural area, mountainous, and forest area. The proposed algorithm is implemented using Matlab. The size of the window used by the proposed method is $5 \times 5$. Larger window may give blurring in edges and point targets and a $3 \times 3$ window may not be statistically independent. The filtered results are compared with the results of the other SAR filters, which include Lee filter, Frost filter, Kuan filter, SRAD filter, NL-mean filter, median filter, and wavelet transform filter. The main purpose of the speckle filter reduces speckle noise and preserves edge details. The evaluating index, equivalent number of look (ENL), is used to evaluate the speckle reduction of the filter. Edge Save Index (ESI) calculates the edge preservation capability of the speckle filter. The parameter equivalent number of look (ENL) is given by

$$\mathrm{ENL} = \frac{\mu^2}{\delta^2}, \tag{22}$$

where $\mu$ is the mean of the image and $\delta$ is the corresponding standard deviation. The greater the value of ENL, better the performance of the speckle reduction.

Edge Save Index (ESI) gives the edge preservation capability of the filter. ESI in horizontal direction is given by (Zhang et al. 2010)

$$\mathrm{ESI}^h = \frac{\sum_{i=1}^{m}\sum_{j=1}^{n-1}|\hat{x}(i,j+1) - \hat{x}(i,j)|}{\sum_{i=1}^{m}\sum_{j=1}^{n-1}|\hat{x}(i,j+1) - \hat{x}(i,j)|}. \tag{23}$$

Similarly, ESI in vertical direction is given by

$$\mathrm{ESI}^v = \frac{\sum_{i=1}^{m-1}\sum_{j=1}^{n}|\hat{x}(i+1,j) - \hat{x}(i,j)|}{\sum_{i=1}^{m-1}\sum_{j=1}^{n}|x(i+1,j) - x(i,j)|}, \tag{24}$$

where $m$ and $n$ are the number of rows and columns, respectively. $\hat{x}$ is the filtered image and $x$ is the speckled image. The values of $\mathrm{ESI}^{\mathrm{h}}$ and $\mathrm{ESI}^{\mathrm{v}}$ should be unity for an ideal filter. Thus, the value closer to the unity indicates better edge preservation.

## 4.1 Experiment on Images

### 4.1.1 Results for SAR Image (Sea Area)

The image in Fig. 2a is acquired over the seaport (image credit: ELTA Systems, Israel) The median filter, Lee filter, Frost filter, Kuan filter, SRAD filter, NL-mean filter, wavelet, and proposed filter are applied to this amplitude multi-look image and their corresponding filtered images are shown in Fig. 2b–i. The size of the amplitude image used for processing is $1024 \times 1364$ which is extracted from the original amplitude image to reduce the runtime. In this study, the window size of the proposed method is $5 \times 5$. The iterations of the SRAD filter are 100 and smoothing step time is 0.025. The degree of filtering ($h$) for the NL mean is 8. The damping factor of the Frost filter is set to 0.5 ($k = 0.5$), here. The ENL and ESI values are tabulated in Table 1. The ENL value is used to evaluate the smoothing. The NL mean has a higher value than the proposed method which shows that these filters have higher smoothing level. By smoothing out the noise, it suppresses dark lines and many point targets. The $\mathrm{ESI}^{\mathrm{h}}$ and $\mathrm{ESI}^{\mathrm{v}}$ values of these filters are quite low. The ENL of the Frost ($5 \times 5$) is comparable with the proposed method, but the ESI values of the proposed method are much higher. Lee filter has the highest edge preserving index. As the Lee filter eludes smoothing near the edges to preserve edges, it leaves a lot of area unfiltered. From the filtered image in Fig. 2c, it can be seen that the Lee filter preserves the strong lines and points. However, the noise near the boundary remains intact.

### 4.1.2 Results for SAR Image (Capitol Building)

The SAR image of the capitol building, Washington is shown in Fig. 3a. The image is four-look intensity image and consists of park area and building (image credit: Sandia National Laboratories, USA). The number of pixels of the image is reduced to $1024 \times 1572$ for evaluation. The ENL and ESI values of the proposed method and other filters are tabulated in Table 2. Figure 3b–i shows the filtered images of the proposed method and others. The window of the proposed method here is $5 \times 5$. The iterations of the SRAD filter are 100 and smoothing step time is 0.025. The degree of filtering ($h$) for the NL mean is 8. The damping factor of the Frost filter is set to 0.5 ($k = 0.5$), here. The ENL value of the NL mean is higher which indicates that it has a better smoothing capability, but it leads to edge blurring by smoothing out the edges. Thus, it has the lowest ESI values. Lee filter preserves edges by inhibiting smoothing near edges. However, the noise near the edges remains unfiltered. Many dark and bright spots can be seen in strong backscattering areas in the Lee-filtered image (Fig. 3c). These isolated dark and bright spots are filtered in the proposed method without affecting the neighbours. The ENL value which is closer to the proposed method is Frost ($3 \times 3$). It smoothes the noise at the expense of fine lines and details. The Frost ($3 \times 3$) has a higher ESI than the Frost ($5 \times 5$) but with the lower ENL. ENL for the SRAD filter can be increased at the expense of ESI. Thus, for the SAR image which consists building block and park area, the proposed method achieves better

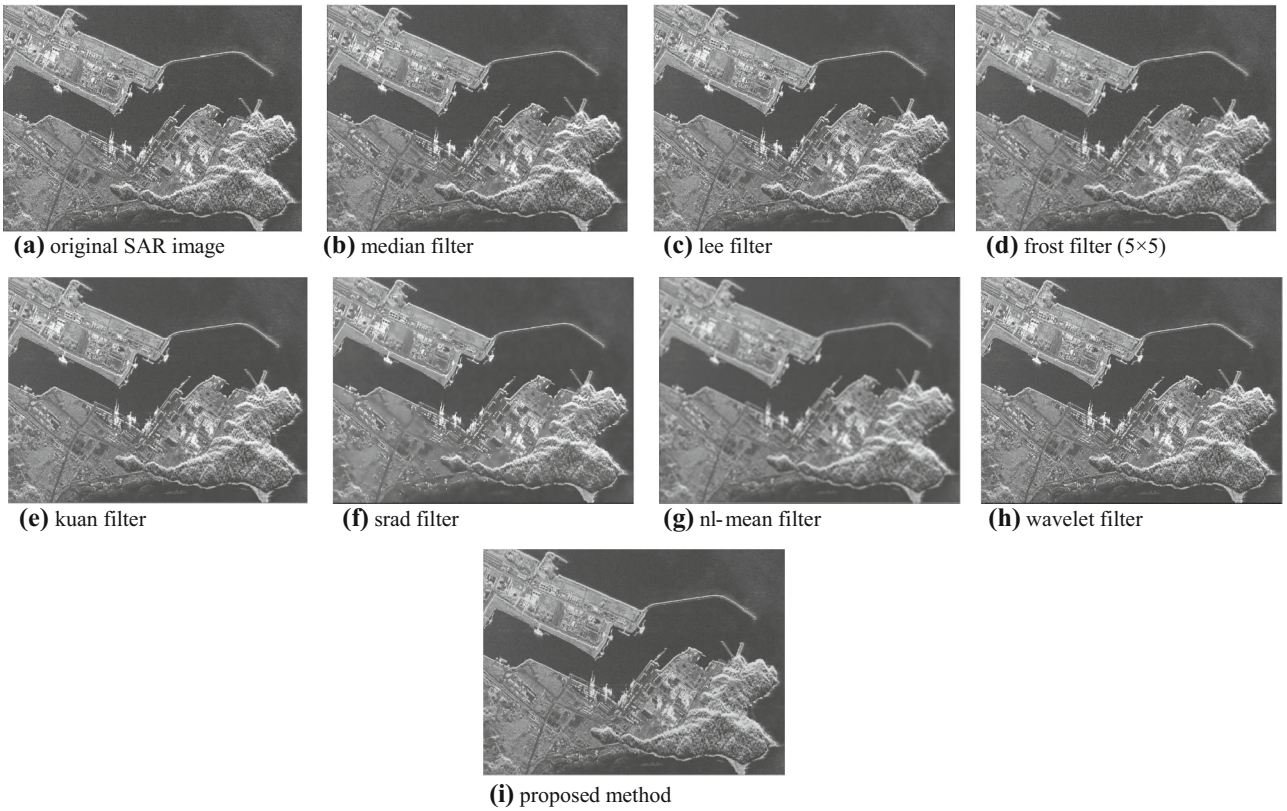


**Fig. 2** SAR image acquired over the sea port (image credit: ELTA Systems, Israel)

**Table 1** Evaluated values for the SAR image (sea area)

| | ENL | ESI | |
|---|---|---|---|
| | | Vertical | Horizontal |
| Median | 4.3699 | 0.4706 | 0.4623 |
| Lee filter | 4.1071 | 0.6631 | 0.6598 |
| Frost (3 × 3) | 4.5699 | 0.4336 | 0.4173 |
| Frost (5 × 5) | 5.0453 | 0.2765 | 0.2566 |
| Kuan | 4.5899 | 0.4294 | 0.4152 |
| SRAD | 4.6771 | 0.3808 | 0.3695 |
| NL mean | 6.1906 | 0.1197 | 0.1040 |
| Wavelet | 4.0544 | 0.5589 | 0.5468 |
| Proposed method | 5.1460 | 0.6530 | 0.6494 |

balance between the noise smoothing and edge and point target preserving.

However, these filters cannot effectively reduce noise when the homogeneousness of the region is low. It can be observed from the filtered images that the proposed method achieves better at balancing the smoothing of noise and preserving the edge information.

#### 4.1.3 Results for SAR Image (Agricultural Area)

The image (Fig. 4a) is acquired over agricultural regions. This 7-look intensity image is taken by RIAN SAR System, IRA, NAS Ukraine. For evaluation, the original image is reduced to 1024 × 1904 pixels. The filtered images of the proposed method and other filters are shown in Fig. 4b–i. The obtained values of ENL and ESI of the proposed method and other filters are summarized in Table 3. As higher ENL values indicate better in noise smoothing, the proposed method performs better in noise smoothing than other filters which are compared except for the SRAD filter, NL mean, and Frost (5 × 5) filters. The SRAD filter, NL mean, and Frost (5 × 5) filters smooth the noise with less preserving details. The proposed method preserves the

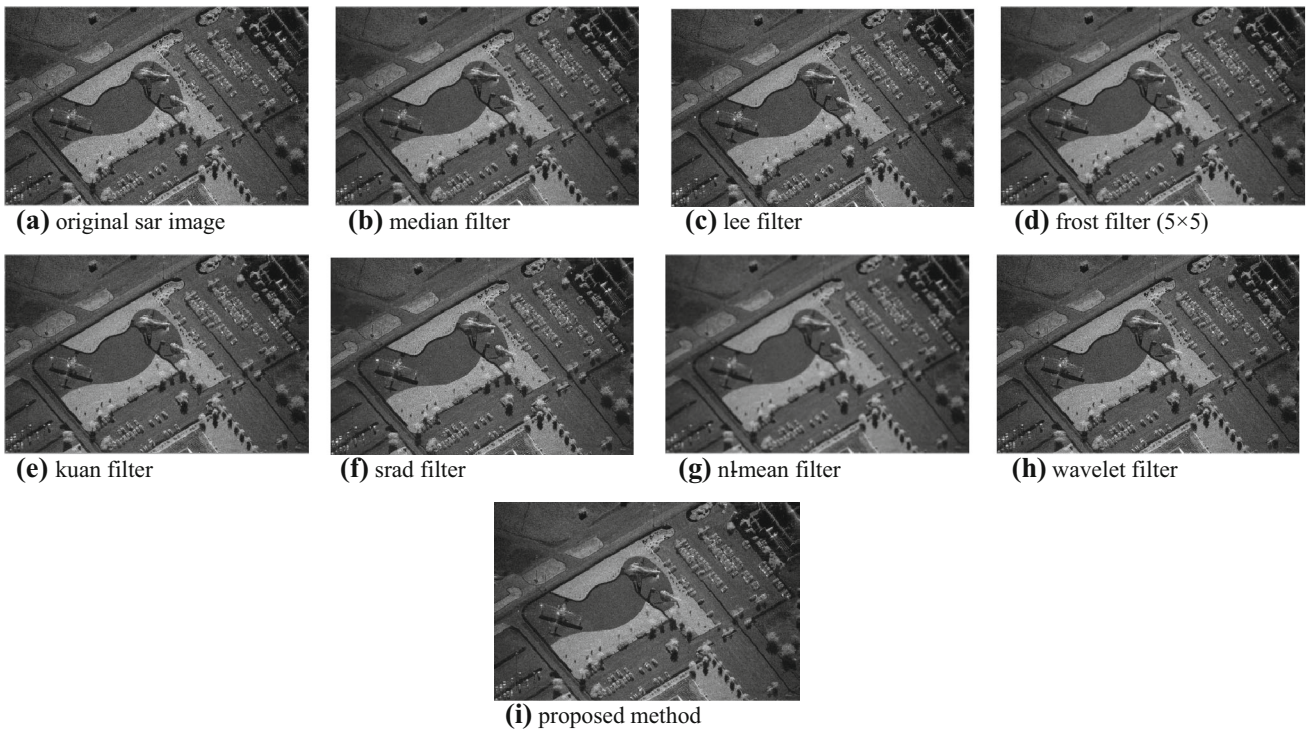


**Fig. 3** SAR image acquired over the Capitol building (image credit: Sandia National Laboratories, USA)

**Table 2** Evaluated values for the SAR image (capitol building)

| | ENL | ESI | |
|---|---|---|---|
| | | Vertical | Horizontal |
| Median | 2.8896 | 0.5072 | 0.4999 |
| Lee filter | 2.7349 | 0.7822 | 0.7791 |
| Frost (3 × 3) | 2.9591 | 0.4886 | 0.4788 |
| Frost (5 × 5) | 3.1852 | 0.2966 | 0.2856 |
| Kuan | 2.9627 | 0.4863 | 0.4702 |
| SRAD | 2.7961 | 0.6121 | 0.6075 |
| NL mean | 3.7035 | 0.1328 | 0.1230 |
| Wavelet | 2.7601 | 0.5985 | 0.5903 |
| Proposed method | 2.9025 | 0.7430 | 0.7396 |

edges and fine details with negligible blurring. The Lee filter has higher ESI values than the proposed method. The noise near the edges is unfiltered in the Lee-filtered image and many dark and bright spots remain in the strong backscattering areas. Unlike the Lee filter, which could not identify the low-gradient terrain, the proposed method smoothes the noise in the terrain area with maintaining the gradient.

## 5 Conclusion

Speckle, the major source of noise in the SAR image, produces fine false structures that degrade the quality of the image. It degrades performance of SAR data analysis techniques and affects the processing tasks such as segmentation and registration. In this paper, an SAR speckle filter is proposed based on the expected value of all the pixel elements in the window with respect to centre pixel. The average of all the expected values in the window replaces the centre pixel. The expected value of the neighbouring pixels is calculated with reference to the centre pixel as it assumes that the original neighbouring pixels' value is closer to the original centre pixel. Experiments are carried out on both air-borne and space-borne SAR images that consist of building block, ocean area, agricultural area, mountainous, and forest area, to study different scattering mechanisms of the image surfaces. Quantitative analysis based on ENL and ESI on these SAR

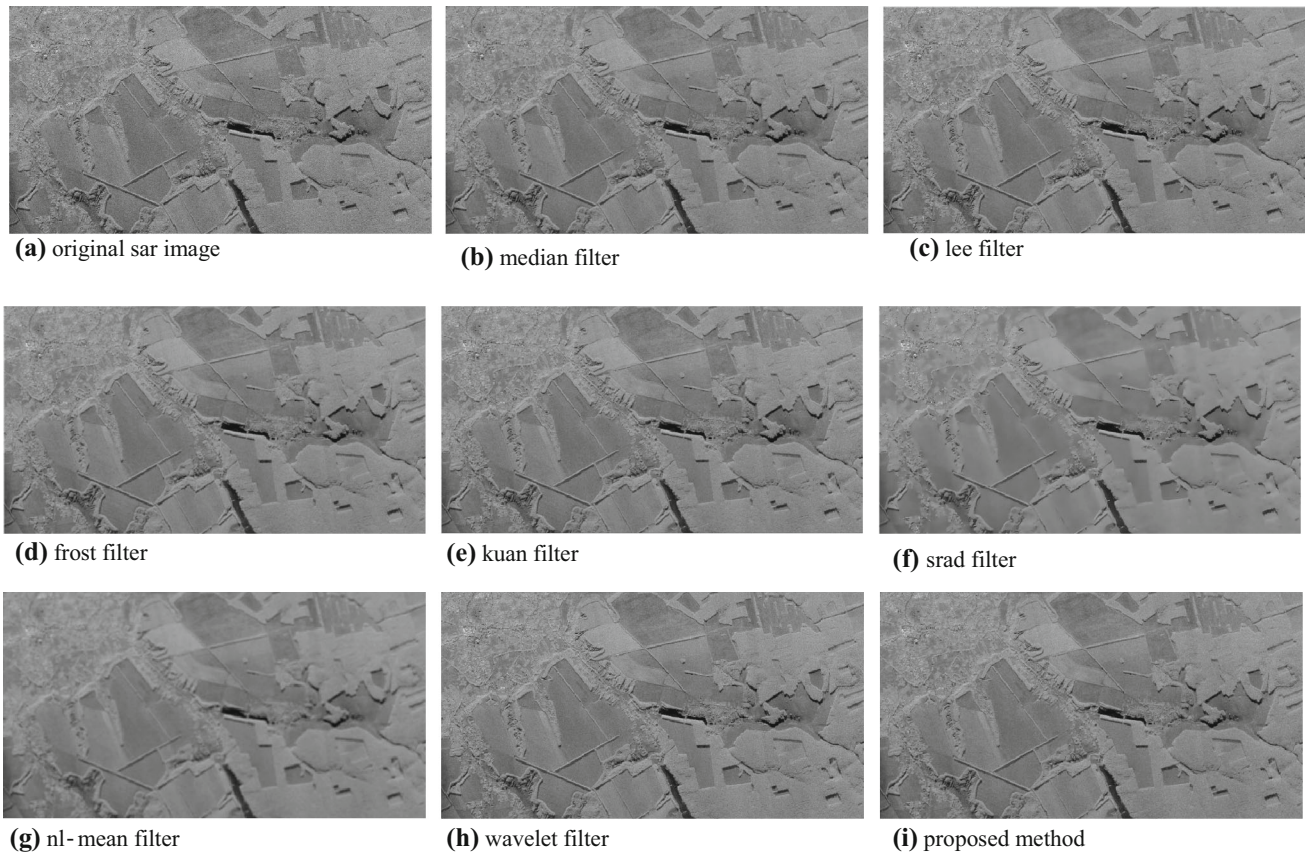


**Fig. 4** SAR image acquired over the over agricultural regions (image credit RIAN SAR System, IRA, NAS Ukraine)

**Table 3** Evaluated values for the SAR image (agricultural area)

| | ENL | ESI | |
|---|---|---|---|
| | | Vertical | Horizontal |
| Median | 23.4390 | 0.3411 | 0.3256 |
| Lee filter | 21.9468 | 0.5122 | 0.5022 |
| Frost (3 × 3) | 24.8035 | 0.3015 | 0.2808 |
| Frost (5 × 5) | 28.5064 | 0.1712 | 0.1533 |
| Kuan | 24.4635 | 0.3083 | 0.2796 |
| SRAD | 29.2825 | 0.1869 | 0.1747 |
| NL mean | 36.9992 | 0.0727 | 0.0614 |
| Wavelet | 21.8337 | 0.3765 | 0.3564 |
| Proposed method | 24.8515 | 0.5449 | 0.5394 |

images shows that the proposed method is more effective in noise smoothing with better preserving edge details and structure information than the other well-known methods. The proposed method is adapted to all the types of image surface as the expected values are calculated based on the probability distribution of the noise.

## References

Achim A, Tsakalides P, Bezerianos A (2003) SAR image denoising via Bayesian wavelet shrinkage based on heavy-tailed modelling. IEEE Trans Geosci Remote Sens 41(8):1773–1784

Achim A, Kuruoglu EE, Zerubia J (2009) SAR image filtering based on the heavy-tailed Rayleigh model. IEEE Trans Image Process 15(9):2686–2693

Argenti F, Lapini A, Bianchi T, Alparone L (2013) A tutorial on speckle reduction in synthetic aperture radar images. IEEE Geosci Remote Sens Mag 1(3):6–35

Buades A, Coll B, Morel J-M (2005) A non-local algorithm for image denoising. In: Computer vision and pattern recognition, CVPR 2005. IEEE Computer Society Conference, vol 2, pp 60–65

Coupé P, Hellier P, Kervrann C, Barillot C (2009) Nonlocal means-based speckle filtering for ultrasound images. IEEE Trans Image Process 18(10):2221–2229

Dainty JCI (1977) The statistics of speckle patterns. Progress Opt 14:1–46

Deledalle C-A, Denis L, Tupin F (2009) Iterative weighted maximum likelihood denoising with probabilistic patch-based weights. IEEE Trans Image Process 18(12):2661–2672

Donoho DL (1995) De-noising by soft-thresholding. IEEE Trans Inf Theory 41(3):613–627

Donoho DL, Johnstone IM, Kerkyacharian G, Picard D (1995) Wavelet shrinkage: asymptopia? J R Stat Soc Ser B (Methodological) 57(2):301–369

Frost VS, Stiles JA, Shanmugam KS, Holtzman JC, Smith SA (1981) An adaptive filter for smoothing noisy radar images. Proc IEEE 69(1):133–135

Gomez L, Munteanu CG, Buemi ME, Jacobo-Berlles JC, Mejail ME (2013) Supervised constrained optimization of Bayesian nonlocal means filter with sigma preselection for despeckling SAR images. IEEE Trans Geosci Remote Sens 51(8):4563–4575

Goodman JW (1976) Some properties of speckle. Opt Soc Am 66(11):1145–1150

Kuan DT, Sawchuk AA, Strand TC, Chavel P (1985) Adaptive noise smoothing filter for images with signal-dependent noise. IEEE Trans Pattern Anal Mach Intell 7(2):165–177

Kuan DT, Sawchuk AA, Strand TC (1987) Adaptive restoration of images with speckle. IEEE Trans Acoust Speech Signal Process 35(3):373–383

Lee J-S (1980) Digital image enhancement and noise filtering by use of local statistics. IEEE Trans Pattern Anal Mach Intell 2(2):165–168

Lee J-S (1981a) Speckle analysis and smoothing of synthetic aperture radar images. Comput Graph Image Process 17(1):24–32

Lee J-S (1981b) Refined filtering of image noise using local statistics. Comput Graph Image Process 15(4):380–389

Lee J-S (1983a) A simple speckle smoothing algorithm for synthetic aperture radar images. IEEE Trans Syst Man Cybernet 13(1):85–89

Lee J-S (1983b) Digital image smoothing and the sigma filter. Comput Vis Graph Image Process 24(2):255–269

Lee J-S (2009) Improved sigma filter for speckle filtering of SAR imagery. IEEE Trans Geosci Remote Sens 47(1):202–213

Lee J-S, Jurkevich L, Dewaele P, Pl Wambacq, Oosterlinck A (1994) Speckle filtering of synthetic aperture radar images: a review. Remote Sens Rev 8(4):313–340

Lee J-S, Grunes MR, De Grandi G (1999) Polarimetric SAR speckle filtering and its implication for classification. IEEE Trans Geosci Remote Sens 37(5):2363–2373

Lee J-S, Ainsworth TL, Wang Y, Chen K-S (2015) Polarimetric SAR speckle filtering and the extended sigma filter. IEEE Trans Geosci Remote Sens 53(3):1150–1160

Leonardo T, Sant'Anna SJS, da Costa Freitas C, Frery AC (2014) Speckle reduction in polarimetric SAR imagery with stochastic distances and nonlocal means. Pattern Recogn 47(1):141–157

Lopes A, Nezry E, Touzi R, Laur H (1990a) Maximum a posteriori speckle filtering and first order texture models in SAR images. In: Geoscience and remote sensing symposium, 1990. IGARSS'90.' remote sensing science for the nineties', 10th annual international, pp 2409–2412

Lopes A, Touzi R, Nezry E (1990b) Adaptive speckle filters and scene heterogeneity. IEEE Trans Geosci Remote Sens 28(6):992–1000

Lopes A, Nezry E, Touzi R, Laur H (1993) Structure detection and statistical adaptive speckle filtering in SAR images. Int J Remote Sens 14(9):1735–1758

Mallat SG (1989) A theory for multiresolution signal decomposition: the wavelet representation. IEEE Trans Pattern Anal Mach Intell 11(7):674–693

Michailovich OV, Tannenbaum A (2006) Despeckling of medical ultrasound images. IEEE Trans Ultrason Ferroelectr Freq Control 53(1):64–78

Novak LM, Burl MC (1990) Optimal speckle reduction in polarimetric SAR imagery. IEEE Trans Geosci Remote Sens 26(2):293–305

Pang B, Xing S, Li Y, Wang Xuesong (2013) Novel polarimetric SAR speckle filtering algorithm based on mean shift. J Syst Eng Electron 24(2):222–223

Parrilli S, Poderico M, Angelino CV, Verdoliva L (2012) A nonlocal SAR image denoising algorithm based on LLMMSE wavelet shrinkage. IEEE Trans Geosci Remote Sens 50(2):606–616

Perona P, Malik J (1990) Scale-space and edge detection using anisotropic diffusion. IEEE Trans Pattern Anal Mach Intell 12(7):629–639

Pratt WK (1975) Median filtering. Image Process Inst Univ Southern California Los Angeles

Shitole S, Sharma M, De S, Bhattacharya A, Rao YS, Krishna Mohan B (2017) Local contrast based adaptive SAR speckle filter. J Indian Soc Remote Sens 45(3):451–462

Simard M, DeGrandi G, Thomson KPB, Benie GB (1998) Analysis of speckle noise contribution on wavelet decomposition of SAR images. IEEE Trans Geosci Remote Sens 36(6):1953–1962

Xie H, Pierce LE, Ulaby FT (2002) SAR speckle reduction using wavelet denoising and Markov random field modelling. IEEE Trans Geosci Remote Sens 40(10):2196–2212

Yamamoto K, Yamaguchi Y, Park S-E, Cui Y, Yamada H (2013) Comparison of speckle filtering methods for POLSAR analysis of earthquake damaged areas. In: Synthetic aperture radar (APSAR), 2013 Asia-Pacific conference on IEEE, pp 358–360

Yousif O, Ban Y (2013) Improving urban change detection from multitemporal SAR images using PCA-NLM. IEEE Trans Geosci Remote Sens 51(4):2032–2041

Yu Y, Acton ST (2002) Speckle reducing anisotropic diffusion. IEEE Trans Image Process 11(11):1260–1270

Zhang W, Liu F, Jiao L, Hou B, Wang S, Shang R (2010) SAR image despeckling using edge detection and feature clustering in bandelet domain. IEEE Geosci Remote Sens Lett 7(1):131–135